On Estimating the Position of Fragments on Rotational Symmetric Pottery *

Robert Sablatnig and Christian Menard
Vienna University of Technology,
Institute of Computer Aided Automation,
Pattern Recognition and Image Processing Group
Treitlstr. 3, 183-2, A-1040 Wien
{sab,men}@prip.tuwien.ac.at, http://www.prip.tuwien.ac.at

Abstract

The archivation of ancient vessel-fragments is a time consuming but important task for archaeologists. The basis for classification and reconstruction is the profile which is the cross-section of the fragment in the direction of the rotational axis of symmetry. Hence the position of a fragment (orientation) on a vessel is important. In this work the estimation of the axis of rotation out of range data by using a Hough inspired method is proposed. In order to avoid outliers the a robust method for estimation of the axis is used. Classification and reconstruction are performed in a bottom-up manner using a description language, which holds all features of the fragment as primitives and all properties among features as relations. Classification of newly found fragments of unknown type is performed by comparing the description of the new fragment with the description of already classified fragments by computing graph similarity. The sub-graph with the highest similarity is then used to reconstruct the complete vessel out of the fragment.

1. Introduction

Usually a large amount of archaeological pottery is found at excavation sites used for 'dating evidence', which is obtained from excavated pottery or its fragments [16]. This evidence is based on the fact that every pot was made or used at a certain time, made at a certain place, and used for a certain purpose. Therefore, every fragment or pot holds the information about when, where, and for what it was made for. This fact places a heavy burden on excavators and recorders of the material since the primary task of pottery research is comparison. This means that pottery must be grouped and recorded in a way that facilitates a comparison. Ceramics are used to distinguish between chronological and ethnic groups and they are used in the economic history to show trading routes and cultural relationships. Especially ceramic vessels, where shape and decoration are exposed to constantly changing fashion, not only allow a basis for dating the archaeological strata, but also provide evidence of local production and trade relations of a community as well as the consumer behavior of the local population.

Figure 1. Drawing of a complete bowl and a fragment of a bowl (from [11]).

There have been several attempts to develop a reliable method of classification, [1, 24], none of them is widely accepted. Figure 1 shows a typical archive drawing which represent bowls. To cope with the fact that this type of archivation prevents a fast comparison of different drawings in order to find two matching fragments, attempts to automate the classification have been introduced [13, 25].None of the prototype systems developed could satisfy the requirements of the archaeologists since the amount of work for the acquisition was not reduced in some cases it was even increased. Furthermore, the accuracy of acquisition was not as high as expected

The manual classification process consists of two steps, the so-called documentation which consists of the determination of the profile, which is the cross-section of the fragment in the direction of the rotational axis of symmetry and the classification which consists of the reconstruction of the

* This work was partly supported by the Austrian Science Foundation (FWF) under grant P13385-INF.

complete vessel out of a fragment with the help of expert knowledge. Since the investigated pottery were made on a rotational plate, the original vessels are assumed to be radially symmetric. The drawing shown in Figure 1 together with different attributes is the output of the manual archiving process.

To automate this process, the profile has to be determined in the same way as in the manual documentation. In order to create the profile the 3-d information of the surface of the fragment has to determined. The acquisition method used for estimating the 3-d shape of a fragment in this work is shape from structured light, which is based on active triangulation [21]. The result is a dense range image. Next, the profile has to be determined in the so-called orientation step. The term orientation describes the exact positioning of the fragment on the original vessel with the help of the axis of rotation. The so generated profile is used to perform the reconstruction and retrieval of fragments of the same type. The reconstruction procedure works if the size of the fragment covers a large part of the original vessel in the vertical direction. The profile is rotated by the original axis of rotation, thus measurements like volume can be estimated. However, if only small fragments (in respect to the vertical size) are available, a reconstruction out of the fragment is not possible. In this case, the fragments have to be classified correctly in order to retrieve matching fragments. A decision model is necessary to make a reconstruction out of small fragments possible.

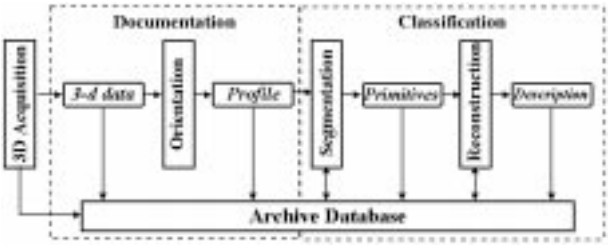

Figure 2. Overview of the approach.

In order to standardize the archivation which is based on the fragment's structure which is stored in an archive database, it can be divided into two main parts, shape features and properties. The classification of shape defines the process where archaeologists distinguish between various features like the profile, the dimensions of the object like diameter and type of surface, whereas the classification of material copes with different characteristics of a fragment like the clay, color and surface properties. Figure 2 shows the automated archivation process schematically: Using the 2.5d-model of the fragment's inner and outer surface, the axis of rotation has to be determined for both surfaces automatically (Section 2). Once the axes are determined the profile section can be generated by registering the two surfaces on one another (see [10] for details). Next, the longest intersection of a plane that is rotated within the rotational axis of the fragment with the surfaces of the fragment is determined (orientation). The profile section of the fragment is the result of this processing step. With the help of this profile, measurements like volume, area, percentage of complete vessel, height, width and so on are computed automatically. The profile and the binarized intensity image of the outer surface are used to draw the archive drawing for non-rim fragments automatically.

In order to make rim fragment drawings, the profile must be segmented into primitives like rim, body, base and so on. This segmentation is be based on mathematical properties of the profile like curvature and length and has to be determined in a classification scheme that uniquely relates primitives to shape properties (Section 3). Next, a classification process tries to find different fragments belonging to the same vessel based on attributes stored in the archive database. After that, the profile of the fragment can be used to reconstruct the original (complete) vessel. This includes the possibility of reconstructing missing parts of the vessel and the search for possible matches of other fragments already stored in the archive with the one that is under consideration (Section 4). We conclude the paper giving an outlook on future work.

2. Orientation of the fragment

In order to determine the position of a fragment on a vessel one important task is the estimation of the axis of rotation. The basis for this axis estimation is a dense range image provided by the range sensor. The acquisition method used for estimating the 3D-shape of a fragment is shape from structured light, which is based on active triangulation [22]. If we have an object of revolution, what in fact is an archaeological pot made on a rotation plate, we can suppose that all intersections I of the surface normals $\vec{\mathbf{n}}$ are positioned along the axis of symmetry R, which is schematically shown in Figure 3.

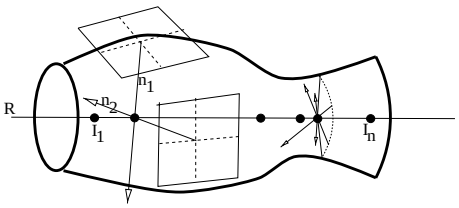

Figure 3. Axis determination using Hough-Space.

Therefore we try to extract a surface of revolution where the curvature of the surface is relatively small. A few approaches to extract volumetric shape descriptors of solids of revolution out of dense range images are reported in Yokoya and Levine [27] and a Hough-based approach to the problem is presented. The Hough transform is a robust and efficient tool for feature extraction [18, 7]. It is based on a voting principle: each point or element will vote for the set of features to which it could belong. This voting principle makes the Hough transform very robust toward noise or outliers [2]. Yokoya and Levine [27] use the center of the principal curvature from first and second partial derivatives of the surface which construct the the so-called focal surface (see [26]). Since our surfaces have a relatively small curvature we adopted this method by using a robust way for the determination of the surface normals, based on planar patches shown in Section 2.1. All surface normals are then clustered in three-dimensional Hough-Space. Instead of detecting point clusters in 2d- projections of the 3d-Hough-Space as performed in [27], we fit a line to the point cluster directly in the Hough-Space as shown in Section 2.2.

2.1. Robust Determination of Surface Normals

For each point on the object, which is represented in the Euclidean space R^3, the surface normal has to be computed which is described in the following:

We consider a planar patch of size $s \times s$. The patch is fitted according to the following equation:

$$ax + by + cz + d = 0\,. \tag{1}$$

This defines a planar patch with normal $\overrightarrow{\mathbf{n}} = (a, b, c)$. The fitting algorithm used is the Total Least Squares (TLS). Let $\mathbf{X}$=$\{\ \mathbf{X_1}, ...\mathbf{X_N}\ \}$, where $\mathbf{X_i} = (x_i, y_i, z_i)$. The TLS minimizes the following expression

$$E_n = \sum_{i=1}^{N} {r_i}^2, \text{where } r_i = \frac{|ax_i + by_i + cz_i + d|}{\sqrt{a^2 + b^2 + c^2}}. \tag{2}$$

It was shown that this approach is equivalent to the MCA or Minor Component Analysis [12]: $\min_{\overrightarrow{\mathbf{n}}} E_n \equiv \mathbf{A}.\overrightarrow{\mathbf{n}} = \lambda_{min}\overrightarrow{\mathbf{n}}$, where $\mathbf{A}$ is the covariance matrix of set $\mathbf{X}$ and λ_{min} is the smallest eigenvalue. The constant d is determined by

$$d = -\overrightarrow{\mathbf{n}}.\frac{1}{N}\sum_{i=1}^{N}\mathbf{X_i}. \tag{3}$$

The main goal is to minimize the distances between the points of the surface and the planar patch. An iterative reweighted algorithm is used to compute the optimal value of the normal and discard outliers. The objective of the algorithm is to achieve:

$$\Delta = \min_{\overrightarrow{\mathbf{n}}} \sum_{i=1}^{s^2} [ax_i + by_i + cz_i + d]^2. \tag{4}$$

In order to minimize the function, we use an iterative scheme. The points are weighted according to their residual [9], a point M_i at iteration k and with residual r_i will have a weight ω_k defined by:

$$\omega_k = \begin{cases} 1 & \text{if } r_i \leq Sa \\ 0 & else \end{cases} \tag{5}$$

where S is the Median Absolute Deviation and a is a tuning constant. The algorithm can be outlined with the initial state $k = 0, \omega_0 = [1...1]$ as follows:

1. compute the surface normal $\overrightarrow{\mathbf{n}}_k$ using weights w_k.
2. compute the residuals r_i with the estimated parameters.
3. compute ω_{k+1} based on r_i.
4. Iterate steps 1. 2. and 3 until convergence.

Once the surface normals for all points are computed the rotation axis can be estimated.

2.2. Axis Estimation

All surface normals $\mathcal{L}_i$ are clustered in three-dimensional Hough-Space: All points belonging to a line $\mathcal{L}_i$ will be incremented in the Hough-Space. Hence the points belonging to a large number of lines (like the points along the axis) will have high counter values. All points in the Hough-Space with a high counter value are defined as maxima. These maxima form the axis of rotation.

In Figure 4 (a) a synthetic range image of a pot is visualized rotated 20 degree around the z axis. In Figure 4 (b) the cross section through the accumulator along the xy-plane in (c) along the xz-plane and in (c) along the yz-plane is shown.

In the next step the line formed by the maxima has to be estimated. There are different techniques to solve this problem. The PCA or principal component analysis [15] is a very popular method, which is used in our case. We have an a-priori knowledge: the maxima point are distributed according to a line (the axis of revolution). The PCA will determine the axis of maximal variance which is in fact the axis of rotation. The accumulator maxima are taken as candidate points for the estimation of the rotation axis. For the set of points $acc(x, y, z)$ a PCA is used to find the optimal axis going through these set of points $\mathcal{M}$ with

$$\mathcal{M} = \{P_i(x, y, z) | g_i = acc(x, y, z) > T_{acc}\}\,, \tag{6}$$

with

$$T_{acc} = s * max(acc), \tag{7}$$

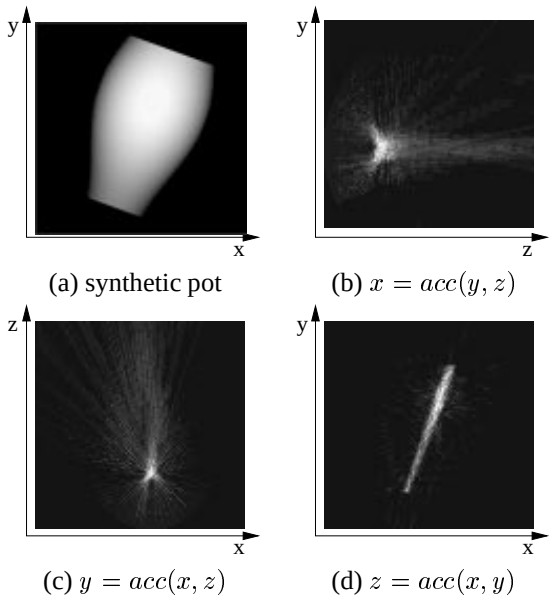

(a) synthetic pot (b) $x = acc(y, z)$

(c) $y = acc(x, z)$ (d) $z = acc(x, y)$

Figure 4. Synthetic range image and cross sections through the accumulator.

where T_{acc} defines a threshold accepting points in the accumulator[1]. In order to estimate the axis the vector $\vec{\mathbf{v}}$ is determined by $\mathbf{A}\vec{\mathbf{v}} = \lambda_{max}\vec{\mathbf{v}}$, where $\mathbf{A}$ is the covariance matrix of set $\mathcal{M}$ and λ_{max} is the largest eigenvalue of $\mathbf{A}$.

A point $\mathbf{G}$ on the axis is determined by using all points in $\mathcal{M}$ with

$$G_{\mathcal{M}} = \frac{\sum\limits_{i\in\mathcal{M}} \tilde{g}_i \, \mathbf{P}_i}{\sum\limits_{i\in\mathcal{M}} \tilde{g}_i}, \text{where } \tilde{g}_i = \begin{cases} g_i & d_i \leq T_d \\ 0 & else \end{cases} \quad (8)$$

and the threshold $T_d = aS$. With the point $\mathbf{G}$ and the vector $\vec{\mathbf{v}}$ the rotation axis is defined, thus a robust version of the complete algorithm can be outlined. The sets $\mathcal{I}_k$ and $\mathcal{O}_k$ are respectively the inlier and outlier sets and the method starts with the initial condition k=0 and $\mathcal{I}_k = \mathcal{M}$ and $\mathcal{O}_k = \{\}$.

1. compute surface normals $\vec{\mathbf{n}}$ for all points of the object.
2. cluster lines $\mathcal{L}_i$ in $acc(x, y, z)$.
3. compute $\vec{\mathbf{v}}_k$ and $\mathbf{G}_{I_k}$ using set $\mathcal{I}_k$.
4. determine the distances d_i of set $\mathcal{M}$ to the axis defined by $\mathbf{G}_{\mathcal{I}_k}$ and $\vec{\mathbf{v}}_k$.
5. update $\mathcal{O}_{k+1}$, $\mathcal{I}_{k+1} = \mathcal{M} - \mathcal{O}_{k+1}$.
6. iterate steps 3., 4. and 5. until convergence or a maximum number of iteration is reached.

[1] In our experiments we used $T_{acc} = s * max(acc)$ with s=0.8.

Using this technique outliers introduced by noisy range data, based on a bad calibration or discretization errors, can be avoided, since in the Hough-Space wrong data points are in the minority and do not build a maximum. Once the axis of rotation is computed, the determination of the profile takes place by intersecting the surface of the fragment with a plane going through the axis of rotation. The longest elongation is supposed to be the profile of the fragment [1].

3. Segmentation of the profile

The segmentation of the profile is done to classify the vessel and to reconstruct missing profile parts. Following this manual strategy, the profile should first be segmented into its parts, the so-called *primitives*, automatically. Our approach to do so is a hierarchical segmentation of the profile into rim, wall, and base by creating segmentation rules based on expert knowledge of the archaeologists and the curvature of the profile. Therefore, the determined profile has to be converted into a parameterized curve [23, 8] and the curvature has to be computed [3, 14]. Local changes in curvature [19] will be the basis for the required rules for segmenting the profile into its primitives: rim, wall, and base. The three primitives are then subdivided into part-primitives, the base for example is divided into flat- and ring-base. Figure 5 shows an archive drawing of a fragment with its profile section divided into various primitives. Up to now this segmentation has been done manually by archaeologists, there are no segmentation standards in archaeology [1].

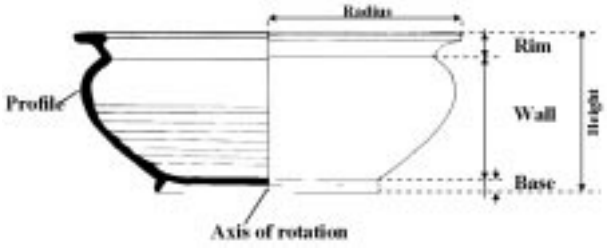

Figure 5. Profile with known primitives.

The segments of the profile are stored in a so-called *description* of the profile. The profile is part of the *fragment model* which can be represented in a *fragment structure*. The fragment structure is formed by its *shape features* (or geometric features like the profile) and its *properties* (or material like clay, color and surface) as shown in Figure 6. The description of the fragment is structured in a *description language* consisting of *primitives* and *relations*. This can be interpreted as a syntactic pattern recognition approach in which the primitives are transformed into the vocabulary and the relations are transformed into a grammar [5].

Within this approach semantic networks [17, 4] can be applied, since semantic networks are labeled, directed graphs where nodes represent objects, sub-objects, or shape primitives and arcs represent relations between them.

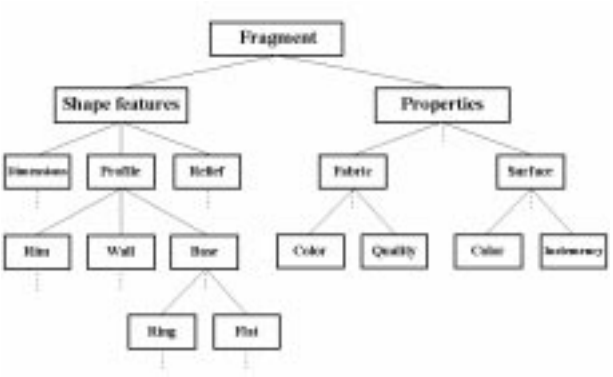

Figure 6. Fragment structure.

The description language, which was originally designed to solve 2-d automatic visual inspection problems [20], was applied and extended in order to solve the profile reconstruction and classification problems. Primitives are a representation of shape features and relations represent the properties. The actual profile contains features which are a representation of shape features. To accomplish classification, primitives are further subdivided into part-models (or part-primitives), the consistency between part-primitives is established by relations among part parameters.

Formally, the description language is a graph $G =< O, R >$, where O denotes the set of nodes and $R = \{O\}$ the set of arcs. A node O consists of different sub-objects or primitives. Each node has different attributes a, with weights w, and a tolerance $T(a)$. Two nodes are in relation according to R. Each relation $< c, d >$ is decomposed into k sub-relations between the same nodes, each with a weight v and a tolerance $T(r)$. Figure 7 shows the graph and the inner structure of nodes and arcs. The shape primitive $S1$ is subdivided into c different shape primitives (such as profile, diameter and the like). For each of these shape primitives n different sub-primitives (such as rim, wall and the like) are defined. The weights w and v are necessary for classification. Each property has a certain weight in order to verify the corresponding description to a given fragment.

The verification of a fragment to its description consists of verifying whether the number and type of features and primitives are the same. Next, attributes and relations are checked whether they match within given tolerances. The verification process is carried out by comparing all attributes of a node and its successors with the model. The confidence for a node can be computed based on the result

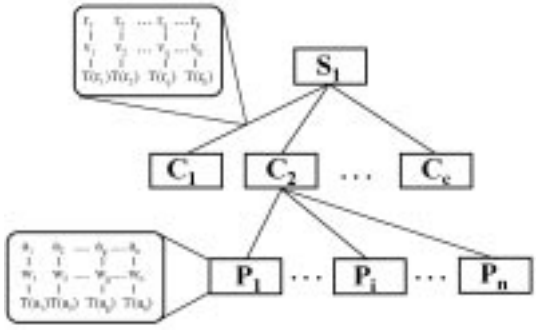

Figure 7. Description language graph.

of the comparison:

$$\text{conf}(p) = \sum_{g=1}^{n} w_g * T(a_g) + \sum_{<p,q> \in \mathbf{R}}^{m} v_{<p,q>} * \text{conf}(q), \quad (9)$$

where w_g are the weights of the attributes of the nodes and $v_{<p,q>}$ the weights of the sub-relations of the arcs. Observe that n, the number of attribute values, and m, the number of arcs, depend on the node p. Moreover, for leaves we have

$$\text{conf}(p) = \sum_{g=1}^{n} w_g * T\ (a_g). \quad (10)$$

This enables us to compute the confidence of a node by summing up the weighted tolerances of each attribute of the node and the overall confidence of the subgraph connected to this node. By computing the consistency for different descriptions the one with the highest confidence value can be chosen if the confidence is above a certain threshold. For a given profile all primitives are represented in the description of the given profile. The segmentation is carried out for all profiles to be classified.

4. Reconstruction results

The goal of the classification process is to find different fragments which belong to the same vessel in order to reconstruct the original vessel, both in electronic and natural ways. After classification, the profile of the fragment can be used to reconstruct the original vessel from its part assemblies. The reconstructed profile together with the axis of rotation are used to create the reconstructed model, fragments can be marked on the reconstructed vessel. Furthermore the 3-d model provides the dimensions of the reconstructed vessel like diameter volume, height, and width. Together with additional information in the archive database the complete description of the fragment is provided.

The orientation algorithm was tested on a set of synthetic and real images. In order to evaluate the accuracy of the

method synthetic range images are used where the axis of rotation is known. To determine the error, the Mean Square Error between the original and the computed axis is determined. The MSE is computed for all points of the axis inside the test object. The MSE of all distances between the estimated and correct axis define the error. In Figure 8 three test objects are visualized, where the estimated axis of rotation is computed in the range image. For each test image the MSE is given according to the position of the original axis. Compared to simple least squares solutions only one wrong surface normal, which is sufficiently far away from the bulk of data can ruin the estimation completely. It can be shown that using our method the axis can be determined even if there are large regions in the range image which are not rotational symmetric (see Figure 8 (b)). Following the evaluation with synthetic range images, range images of fragments were tested. One example is depicted in Figure 8 (c). Although there exist regions in the range image where no depth information is available (black areas) due to occlusions, highlights, and shadows, the axis is determined and the MSE is estimated.

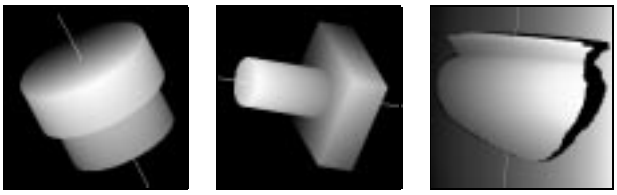

(a) MSE=0.16 (b) MSE=0.22 (c) MSE=0.23

Figure 8. Axis determination for synthetic and real range data.

To find out how well the method is working on real data we used a totally symmetric small flowerpot with known dimensions and took a fragment which covered approximately 25% of the original surface. The range images of the front- and back-view consisted of approximately 10.000 surface points each (Figure 9a,b). The MSE for these two examples was 0.32 and 0.28 respectively. Figure 9c and Figure 9d show the front- and the backview of an archeological fragment, the MSE for the frontview was 0.22, for the backview the MSE was 0.35 due to occlusions in the range image and a diversion of the computed axis in the direction of the bottom of the fragment.

With the help of the axis of rotation the surfaces of the fragments are registered (see [10]). From the 3d-object profiles of the fragments were computed and manually segmented into the profile primitives. The parameters of the primitives and their relations were stored in the description language, all operations for classification and reconstruction can be executed on this graph structure. The advantage

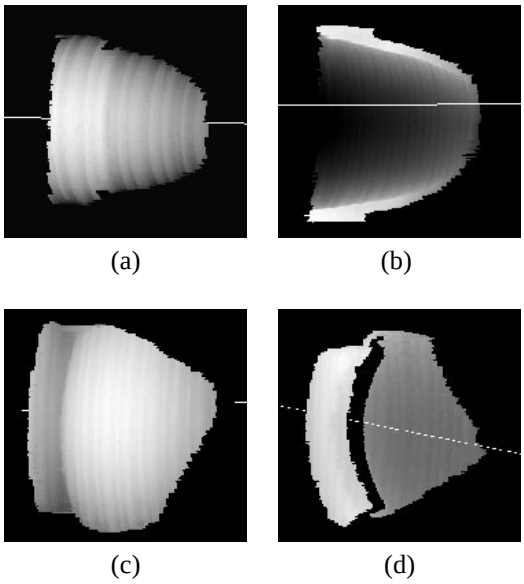

(a) (b) (c) (d)

Figure 9. Front- and back-view and their axis of rotation of a flowerpot (a,b) and an archaeological fragment (c,d).

of a description language lies in the uniqueness of representation; different fragments result in different descriptions, similar fragments result in similar descriptions. The shape is subdivided into c different shape primitives (such as profile, diameter and the like). For each of these shape primitives n different sub-primitives (such as rim, wall, and the like) are defined. Since manual segmentation of the profile varies, tolerances and weights within the description are used. The tolerance for profile primitives is 2110local thickness which has a weight of 0.7. These values where defined empirically so far.

Two fragments of the same vessel were taken to test the retrieval (Figure 10 describes this example). Each fragment has a unique number when archived. Together with all attributes the fragment is stored in the description. The lower left hand side of (Figure 10 shows a profile, which was classified as bowl and separated into edge (E048), border (B012), and ringbase (R145). These primitives are the basis for the classification and reconstruction process.

On the top left hand side of Figure 10 the intensity image of a fragment which is not yet classified is depicted. Following the 3d-acquisition and the orientation (i.e. the determination of the rotational axis) the profile is generated. At this stage the type of the vessel is not yet known. The profile is segmented into its primitives and the according attributes like color, surface, and dimensions are determined. In order to classify the fragment (find the vessel in the database that matches the fragment) the generated de-

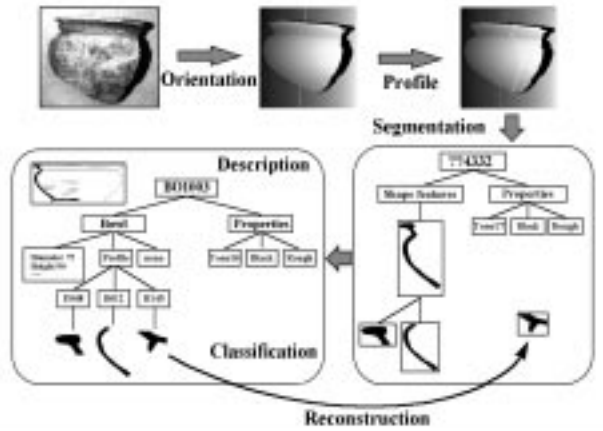

Figure 10. Reconstruction using segmented profile of the fragment and description of known vessels.

scription is compared with already existing descriptions. If the profile primitives of the fragment can be found in the description and other attributes are matching within a given tolerance the type of the fragment can be classified as bowl. Furthermore, missing parts of the fragment (like the base in this case) can be reconstructed based on the already stored information.

5. Conclusion and outlook

In archaeology a number of papers tackle the problem of objective manual classification, although no standard can be determined, each country and region has its own standard (see for instance [1, 6]). One computer based approach [25] tried to give a solution to the classification problem by approximate cross-section by 2-d curves, due to the errors introduced by the acquisition system and the curve fitting this solution was not accepted by archaeologists since matching profiles could not be found in a robust manner.

In contrast to this subjective approaches, our primitive-based approach gives the possibility to relate different profiles to common primitives or sub-primitives. Therefore, it is possible to reconstruct different profiles out of one primitive, the expert has the possibility to choose the most relevant. Furthermore the acquisition and orientation is fully automated, a robust determination of the axis of rotation allows a robust computation of the profile used to classify the fragment. This profile is segmented into primitives. The advantage of this method is that part similarities of profiles can be detected and complete vessels can be reconstructed based on the already stored data in the archive database. The bottom-up design using a description language for the reconstruction process makes a detection of similar fragments in the database possible, because the matching process starts with the comparison of the entire primitives with already existing relations.

Future work will be guided towards automated segmentation of the entire profile using mathematical models and developing an adaptive strategy for orientation using a hierarchical structured Hough-space to be more efficient in determining maxima.

References

[1] W. Adams and E. Adams. *Archaeological Typology and Practical Reality. A Dialectical Approach to Artifact Classification and Sorting*. Cambridge, 1991.

[2] D. Ballard and C. Brown. *Computer Vision*. Prentice Hall, 1982.

[3] J. Bennett and J. MacDonald. On the Measurement of Curvature in a Quantized Environment. *IEEE Trans. on Computer*, 24:803–820, 1975.

[4] A. Darwish and A. Jain. A Rule-based Approach for Visual Pattern Inspection. *IEEE Trans. on PAMI*, 10(1):56–58, 1988.

[5] K. Fu. Syntactic Pattern Recognition. In T. Young and K. Fu, editors, *Handbook of Pattern Recognition and Image Processing*, pages 84–117. Academic Press, 1986.

[6] J. Gardin. *Code pour l'analyse des formes de poteries*. Paris, 1985.

[7] M. Hoffelder, K. Sauer, and J. Rigby. A Hough Transform Technique for Detection of Rotationally Invariant Surface Features. In *Proc. of 1st. Intl. Conference on Image Processing, Austin, Texas*, pages 944–948, 1994.

[8] Z. Hu and S. Ma. The Three Conditions of a Good Line Parameterization. *Pat. Rec. Let.*, 16:385–388, 1995.

[9] P. J. Huber. *Robust Statistics*. Wiley, New York, 1981.

[10] M. Kampel and R. Sablatnig. A Model-based Approach to Range Image Registration. In M. Vincze, editor, *Robust Vision for Industrial Applications, Proc. of the 23rd Workshop of the Austrian Association for Pattern Recognition (OEAGM)*, volume 128, pages 109–117. Schriftenreihe der OCG, 1999.

[11] P. Kenrick. *Rim-forms of some Relief-decorated Vessels in Italian Terra Sigillata*. Conspectus formarum terrae sigillatae italico modo confectae. Bonn, 1990.

[12] E. O. L. Xu and C. Suen. Modified Hebian Learning for Curve and Surface Fitting. *Neural Networks*, 5(3):441–457, 1992.

[13] U. Lübbert and U. Kampffmeyer. Forschungsprojekt ARCOS: Ein Rechner und Programmsystem für die Archäologie. *Archäologie in Deutschland*, (Heft 1/89):36–40, 1989.

[14] J. Matas, Z. Shao, and J. Kittler. Estimation of Curvature and Tangent Direction by Median Filtered Differencing. In *Proc. of 8th ICIAP*, pages 83–88, 1995.

[15] E. Oja. *Subspace Methods of Pattern Recognition*. John Wiley, 1983.

[16] C. Orton, P. Tyers, and A. Vince. *Pottery in Archaeology*, 1993.

[17] M. Quillian. Semantic Memory. In M. Minsky, editor, *Semantic Information Processing*, Cambridge, 1968. M.I.T. Press.

[18] P. T. R.K Yip, W.C Lam and D. Leung. A Hough Transform Technique for the Detection of Rotational Symmetry. *Pat. Rec. Let.*, 15(9):919–928, 1994.

[19] A. Rosenfeld and A. Nakamura. Local Deformations of Digital Curves. *Pat. Rec. Let.*, 18(7):613–620, July 1997.

[20] R. Sablatnig. *A Highly Adaptable Concept for Visual Inspection*. PhD thesis, TU-Vienna, Inst. f. Automation, Pattern Recognition and Image Processing Group, 1997.

[21] R. Sablatnig and C. Menard. Computer based Acquisition of Archaeological Finds: The First Step towards Automatic Classification. In P. M. Mariotti, editor, *Proceedings of the 3rd International Symposium on Computing and Archaeology, Rome*, volume 1, pages 429–446, 1996.

[22] R. Sablatnig, C. Menard, and P. Dintsis. Bildhafte, dreidimensionale Erfassung von archäologischen Fundgegenständen als Grundlage für die automatisierte Klassifikation. In O. Stoll, editor, *Computer & Antike*, volume 3, pages 59–84. Scripta Mercaturae Verlag, 1994.

[23] A. Shoukry and A. Amin. Topological and Statistical Analysis of Line Drawings. *Pat. Rec. Let.*, 1:365–374, 1983.

[24] C. Sinopoli. *Approaches to Archaeological Ceramics*. New York, 1991.

[25] C. Steckner. Das SAMOS Projekt. *Archäologie in Deutschland*, (Heft 1):16–21, 1989.

[26] N. Yokoya and M. Levine. Volumetric Descriptions of Solids of Revolution in a Range Image. In *Proc. of 10th. Intl. Conference on Pattern Recognition, Atlantic City, NJ*, pages 303–308, 1990.

[27] N. Yokoya and M. Levine. Volumetric Shapes of Solids of Revolution from a Single-View Range Image. *Computer Vision, Graphics and Image Processing: Image Understanding*, 59(1):43–52, 1994.